FEMS Microbiology Ecology, 92, 2016, fiw105

doi: 10.1093/femsec/fiw105
Advance Access Publication Date: 18 May 2016
Research Article

RESEARCH ARTICLE

Promiscuous and specific bacterial symbiont acquisition in the amoeboid genus *Nuclearia* (Opisthokonta)

Sebastian Dirren and Thomas Posch*

Limnological Station, Department of Plant and Microbial Biology, University of Zurich, Seestrasse 187, CH-8802 Kilchberg, Switzerland

*Corresponding author: Limnological Station, Department of Plant and Microbial Biology, University of Zurich, Seestrasse 187, CH-8802 Kilchberg, Switzerland. Tel: 0041-44-634-9224; Fax: 0041-44-634-9225; E-mail: posch@limnol.uzh.ch

One sentence summary: Many amoeboid species of the genus *Nuclearia* (Opisthokonta) feed on filamentous cyanobacteria and live together with ectosymbiotic and/or endosymbiotic bacteria.

Editor: Julie Olson

ABSTRACT

We isolated 17 strains of the amoeboid genus *Nuclearia* (Opisthokonta) from five Swiss lakes. Eight of these nucleariid isolates were associated with bacterial endosymbionts and/or ectosymbionts. Amoebae were characterized morphologically and by their 18S rRNA genes. Phylogeny based on molecular data resulted in four established monophyletic branches and two new clusters. A heterogeneous picture emerged by highlighting nucleariids with associated bacteria. Apart from one cluster which consisted of only isolates with and three groups of amoebae without symbionts, we also found mixed clusters. The picture got even more 'blurred' by regarding the phylogeny of symbiotic bacteria. Although seven different bacterial strains could be identified, it seems that we still are only scratching the surface of symbionts' diversity. Furthermore, types of symbioses might be different depending on host species. Strains of *Nuclearia thermophila* harboured the same endosymbiont even when isolated from different lakes. This pointed to a specific and obligate interaction. However, two isolates of *N. delicatula* were associated with different endosymbiotic bacteria. Here the symbiont acquisition seemed to be rather promiscuous. This behaviour regarding symbiotic associations is especially remarkable considering the phylogenetic position of these basal opisthokonts.

Keywords: bacteria-protist symbioses; ectosymbionts; endosymbionts; *Nuclearia*; Nucleariidae; glycocalyx

INTRODUCTION

Intimate associations between unicellular or invertebrate eukaryotes and prokaryotes are ubiquitous, and their importance for the evolution of 'higher' life forms is increasingly recognized (Smith 1989; McFall-Ngai *et al.* 2013; Alegado and King 2014; Kiers and West 2015). We can intuitively argue that the probability of interactions increases if the spatial distance between hosts and potential symbionts is small, which is often the case for protists and bacteria. Knowing that such interactions are manifold, we use the term symbiosis in a very general way. We call the phenomenon of a close association of dissimilar organisms a 'symbiosis', thus we follow the original definition of this term by de Bary (see Appendix 1 in Paracer and Ahmadjian 2000). On an evolutionary scale, symbioses between eukaryotes and prokaryotes may emerge and disintegrate constantly and only a minute part will turn into 'stable associations'. The most stated and intensively studied examples are mitochondria and plastids that originated from the endosymbiosis of a host cell

Received: 28 January 2016; **Accepted:** 15 May 2016

with alphaproteobacteria (Thrash *et al.* 2011) and cyanobacteria (Rodríguez-Ezpeleta *et al.* 2005), respectively. Beside the fundamental functions of respiration and photosynthesis, we know several traits which bacterial symbionts may provide to their eukaryotic hosts, e.g. they can be important for the host's nutrition, defence, competition and adaption to the environment (Gast, Sanders and Caron 2009). Associated bacteria can also be involved in the production (Freeman *et al.* 2012) or degradation of secondary metabolites including toxins (Kikuchi *et al.* 2012; Dirren *et al.* 2014).

Here we focus on members of the amoeboid genus *Nuclearia* (Opisthokonta, Nucleariidae) which can live in symbiosis with ecto- and endosymbiotic bacteria. *Nuclearia* is a single genus in the family Nucleariidae which is a sister group to Fungi (Zettler *et al.* 2001; Steenkamp, Wright and Baldauf 2006; Liu *et al.* 2009). As far as we know, there is only one documented case of an opisthokont protist with prokaryotic symbionts. Wylezich *et al.* (2012) described the choanoflagellate *Codosiga balthica*, which harboured two different endosymbiotic bacteria inside the cytoplasm. This lack of evidence is remarkable considering the importance of symbiotic interactions for multicellular opisthokonts. Nucleariid amoebae are usually surrounded by a glycocalyx (Moran, Gupta and Joshi 2011; Ouwerkerk, de Vos and Belzer 2013), which can be colonized by ectosymbiotic bacteria (Artari 1889; Cann and Page 1979; Patterson 1984; Cann 1986). In a previous study, we characterized *Nuclearia* sp. strain N (hereafter named *Nuclearia thermophila* strain N) which harboured the bacterial ectosymbiont (*Paucibacter toxinivorans*) nicely arranged inside the glycocalyx (Dirren *et al.* 2014). The interaction between *N. thermophila* strain N and this prokaryote seemed to be specific and stable.

Multicellular organisms usually are associated with more than one bacterial species. Ectosymbionts form entire assemblages which are designated as microbiota of the respective host. The microbiota of very 'simple' animals like the cnidarians *Hydra* (Fraune and Bosch 2007; Franzenburg *et al.* 2013) and corals (Lema, Bourne and Willis 2014) seem to be relatively distinct and even species specific. In higher animals including humans (Huttenhower *et al.* 2012), the microbiota is more diverse and variations between individuals within the same population are pronounced. However, in contrast to the taxonomic variability, the functional roles of such assemblages seem to be conserved. Thus, composition and function of the microbiota is essential for the organism's well-being. A multitude of diseases are consequently caused by regime shifts to unhealthy and unstable states (Lozupone *et al.* 2012). The 'simplicity' of the *Nuclearia* system could be a great benefit for the fundamental understanding of interactions of prokaryotes with their opisthokont hosts.

Symbiotic interactions of Nucleariidae are not restricted to ectosymbiotic associations but amoebae may additionally harbour bacterial endosymbionts. For example, *N. radians* (described as *Nucleosphaerium tuckeri* by Cann and Page 1979) may be associated with ectosymbiotic and endosymbiotic bacteria. In recent studies, the rickettsial endosymbiont of *N. pattersoni* (Dykova *et al.* 2003) and *Candidatus* Endonucleariobacter rarus (Dirren *et al.* 2014) of *N. thermophila* strain N were characterized. Endosymbiotic bacteria are not at all as common in higher life forms as ectosymbionts. The barrier for bacteria to enter metazoans' cells is rather rigid and well protected (e.g. by the immune system). In vertebrates, mainly pathogens are able to enter cells causing infections and pathological states (Casadevall 2008). From an evolutionary point of view, this is of great interest as multicellular organisms seem to 'outsource' their bacterial associations to preserve their integrity. Consequently, the glycocalyx can be regarded as a kind of 'external organ' harbouring the symbiotic assemblage. This arrangement not only allows benefiting from the microbiota but also ensures a minimal physical distance and thus protection (Fraune *et al.* 2015).

To sum up, from a phylogenetic perspective, Nucleariidae might be good model organisms to verify hypotheses about symbioses in general. In order to study these interactions, it is the first step to elucidate the diversity of Nucleariidae and to characterize in parallel their symbionts. In this study, (i) we report on the morphology and taxonomic affiliation (18S rRNA genes) of 17 *Nuclearia* strains; (ii) all isolates were screened for bacterial symbionts both in the glycocalyx and inside amoebae; (iii) finally, we focused on symbionts of *N. delicatula* and *N. thermophila* strains, and analysed the ultrastructure and the intracellular localization of endosymbiotic bacteria via transmission electron microscopy (TEM). Additionally, we sequenced the bacterial 16S rRNA genes for phylogenetic analyses.

METHODS

Strains and cultures

A total of 17 *Nuclearia* strains were isolated from benthic and pelagic water samples of five Swiss lakes (Table 1). Single cells were picked with a glass pipette and washed in sterile water to generate monoclonal xenic amoebal cultures. Finally, isolates were cultured in autoclaved mineral water (Cristalp) and the cyanobacterium *Planktothrix rubescens* was added as sole food source. *Planktothrix rubescens* BC 9307 was isolated from Lake Zurich (Walsby, Avery and Schanz 1998) and is kept as axenic stock culture. *Nuclearia* cultures were maintained at a 12 h light (irradiance: 5–15 μmol m^{-2} s^{-1})/12 h dark cycle in Tissue Culture Flasks 25 cm^2 (TPP) at 18°C. Cultures were fortnightly renewed by adding 1 ml of the axenic cyanobacterial stock culture to 10 ml of new culture medium inoculated with 200 μl of an older culture. For all analyses, we included the dataset about *N. thermophila* strain N and its bacterial ectosymbiont *P. toxinivorans* strain SD41 (HG792253), originating from our previous study (Dirren et al. 2014). *Nuclearia delicatula* strain G (CCAP 1552/6), *N. moebiusi* strain K (CCAP 1552/7), *N. thermophila* strain N (CCAP 1552/5) and *N. pattersoni* strain A2 (CCAP 1552/8) were deposited in the Culture Collection of Algae and Protozoa (CCAP).

Morphological analysis and cladistic tree

Morphological characters were observed by light microscopy on living specimens. Features like multinucleate/uninucleate, evident/not evident nucleolus and branching of filopodia were observed when cells adapted a flattened form under the compression of the cover slip. Cells were considered 'spherical' if floating individuals in the water column could be observed (even if they were not always 'perfect' spheres). Strains were classified as being able to adapt a 'flattened form' when cells have ever attached to and moved on surfaces. The formation of syncytia was defined as the fusion of two or more cells. In addition, we checked all culture flasks for the appearance of cysts. The glycocalyx was either seen with phase contrast as translucent halo surrounding cells or after staining with Alcian blue. Ectosymbionts were defined as bacteria inside the glycocalyx located close to the cell membrane (loosely attached bacterial cells on the outer border of the glycocalyx were not classified as symbionts). Endosymbionts were detected with epifluorescence microscopy after DAPI staining and by in situ hybridization (CARD-FISH). The body diameter of spherical cells was

Table 1. Features of *Nuclearia* isolates. The following features were observed for all strains and thus are not listed: spherical form, flattened form, nucleolus, glycocalyx and branching of filopodia. If not stated otherwise, strains were isolated from benthic samples. Strains are listed according to the phylogenetic tree shown in Fig. 1A. In case that bacterial symbionts could be identified with CARD-FISH, the adequate oligonucleotide probes are listed (see Table 2 for probes abbreviations). Lake Zurich: 47°19′11.5″N, 8°33′10.1″E, Lake Hallwil: 47°18′16.3″N, 8°13′03.3″E, Lake Sempach: 47°08′15.8″N, 8°08′25.8″E, Lake Baldegg: 47°11′38.9″N, 8°15′46.6″E, Lake Soppi: 47°05′25.6″N, 8°04′51.5″E.

Nuclearia sp. strain	Nucleus	Ectosymbiont	Endosymbiont	Cysts	Mean size (range); *n* (sizes in μm)	18S rRNA sequence	Isolation date; source
N. delicatula strain G	Multinucleate	Bu154	Del1424 and Le827	–	26 (17.2–45.8); $n = 100$	LN875119	Oct 2012; Lake Zurich
N. delicatula strain D	Multinucleate	+ (lost)[a]	AlRick85	–	20.4 (10.7–82.2); $n = 133$	LN875118	Feb 2012; Lake Zurich
N. delicatula strain S4	Multinucleate	+ (lost)[a]	Del1424	–	24.5 (12.8–104.8); $n = 100$	LN875117	Oct 2014; Lake Sempach
N. delicatula strain D4	Multinucleate	+ (lost)[a]	Del1424	–	24 (13.8–42.6); $n = 100$	LN875116	Oct 2014; Lake Sempach
N. delicatula strain B6	Multinucleate	+ (lost)[a]	–	–	26.7 (15–45.6); $n = 107$	LN875115	Sep 2014; Lake Hallwil
N. moebiusi strain K	Uninucleate	–	–	–	9.8 (3.8–15.1); $n = 100$	LN875108	Oct 2012; Lake Zurich
N. thermophila strain B1	Uninucleate	–	–	+	15.4 (9.5–23.2); $n = 100$	LN875121/22	Nov 2013; Lake Zurich
N. thermophila strain D6	Uninucleate	–	CoNuc67	+	15.7 (9.4–22.7); $n = 100$	LN875109	Sep 2014; Lake Hallwil
N. thermophila strain A	Uninucleate and multinucleate syncytia	+ (lost)[a]	CoNuc67	+	17.7 (9.8–28.3); $n = 270$	LN875106	May 2011; Lake Zurich
N. thermophila strain N	Uninucleate and multinucleate syncytia	Pauci995	CoNuc67	+	16.4 (7.2–29); $n = 448$	HG530253	Aug 2011; Lake Zurich
Nuclearia sp. strain B3	Uninucleate	–	–	–	8.7 (5–14.2); $n = 100$	LN875120	Sep 2014; Lake Baldegg[b]
Nuclearia sp. strain A5	Uninucleate and multinucleate syncytia	–	–	–	9.2 (5.4–15.4); $n = 100$	LN875107	Sep 2014; Lake Hallwil[b]
N. pattersoni strain B4	Uninucleate	–	–	+	8.4 (5.4–15.3); $n = 100$	LN875111	Oct 2014; Lake Soppi[b]
N. pattersoni strain A2	Uninucleate	–	–	+	9.9 (6.5–17.8); $n = 100$	LN875110	Sep 2014; Lake Baldegg[b]
Nuclearia sp. strain NZ	Uninucleate	–	–	–	16.7 (10.6–28.4); $n = 100$	LN875112	Oct 2012; Lake Zurich[b]
Nuclearia sp. strain A1	Uninucleate	–	–	–	12.3 (8.2–18.3); $n = 106$	LN875113	Oct 2014; Lake Sempach
Nuclearia sp. strain D1	Uninucleate	–	–	–	11.9 (6.9–19.4); $n = 124$	LN875114	Oct 2014; Lake Sempach

[a] Amoebae lost bacterial ectosymbionts during long-term cultivation.
[b] Amoebal strains were isolated from the pelagic zone of the respective lake.

measured more than 3 months after isolation of the strains. Only for *N. thermophila* strain D6, additional measurements were taken right after isolation. For calculations of the cladistic tree, morphological characters were judged as either present or absent and each strain was attributed to one of three size classes: 1. x < 13 μm; 2. 13 μm < x < 20 μm; 3. x > 20 μm. The cladistic tree (Jaccard's similarity coefficient) was calculated with the Add-In software XLSTAT (Addinsoft).

Sequencing of the 18S rRNA genes (Nucleariidae)

DNA was extracted from aliquots (1.5 ml) of *Nuclearia* cultures with the GenElute Bacterial Genomic DNA Kit (Sigma). PCR with GoTaq® Green Master Mix (Promega) and the eukaryote-specific primers Euk328f and Euk329r (Moon-van der Staay, De Wachter and Vaulot 2001) were used to amplify the 18S rRNA genes. If gel elecrophoresis resulted in the detection of bands of expected size, PCR products were purified with QIAquick PCR Purification Kit (Qiagen) and Sanger sequenced with ABI BigDye chemistry on an ABI 3130x Genetic Analyzer (Applied Biosystems). In order to sequence the entire amplicons, the additional primers SR2f, SR2r, SR4f, SR6f, SR6r, SR8f, SR8r, SR10f and SR10r (Nakayama *et al.* 1998) were used. In seven cases (strains G, D, S4, D4, B6, B1 and B3), the direct sequencing was not successful. Here 18S rRNA genes were again amplified from the extracted DNA with Platinum PCR Super Mix High Fidelity (Invitrogen) and the primers Euk328f and Euk329r. Subsequently, PCR products were purified as mentioned above and cloned into *Escherichia coli* using a pGem-T Vector (Promega) according to the manual. Clones were screened for expected size inserts with the plasmid primers M13f and M13r. Positive clones were grown in liquid cultures, and plasmids were purified with GenElute Five-Minute Miniprep Kit (Sigma). Inserts of plasmids were sequenced in the same way as PCR products but plasmid primers were used instead of Euk328f and Euk329r.

Sequencing of the 16S rRNA genes (symbionts)

Two 16S rRNA gene clone libraries were constructed from *N. delicatula* strain D and strain G, respectively. About 130 *Nuclearia* cells were picked with a micropipette and washed in sterile water. After three freeze–thaw cycles, DNA was extracted with GenElute Bacterial Genomic DNA Kit (Sigma). Extracted DNA served then as template for amplification of 16S rRNA genes with Platinum PCR Super Mix High Fidelity (Invitrogen) and the primers GM3f and GM4r (Muyzer and Ramsing 1995). After purification of PCR products and ligation into the pGem-T Vector (Promega), they were cloned following the manufacturer's protocol. Positive *E. coli* clones were detected by screening with plasmid primers (size ~1.6 kbp) and their plasmids purified as described above. Sequencing of inserts was done with plasmid primers and the additional primer GM1f (Muyzer and Ramsing 1995). Partial 16S rRNA genes of the endosymbiont *Candidatus* Endonucleariobacter rarus from *N. thermophila* strain A and strain D6 were sequenced directly. The sequence of the probe CoNuc67 (Table 2) was used to design a specific primer (P1_CoNuc_f 5′-TAACAGAGTGTGTAGC-3′). PCR amplification with GoTaq Green Master Mix (Promega) was done with extracted DNA from these cultures using the forward primer P1_CoNuc_f and the reverse primer GM4r (positive control: ext. DNA from *N. thermophila* strain N; negative control: ext. DNA from *N. thermophila* strain B1). Subsequently purified PCR products were directly sequenced with the primers P1_CoNuc_f and GM4r as described above (LN875086–LN875088).

Table 2. Specific CARD-FISH probes applied in this study. Affiliations of the target bacteria to major taxonomic groups are given in brackets: AlRick85 (Alphaproteobacteria), Bu154 and Pauci995 (Betaproteobacteria), Del1424 (Deltaproteobacteria), CoNuc67 and Le827 (Gammaproteobacteria).

Probe (Reference)	Sequence (5′ to 3′)	Specificity	FA in %[a]	Hits in RDP[b]/Δ FA in % to the non-targets[c]
CoNuc67 (Dirren *et al.* 2014)	ATTGCTACACACTCTGTTACCG	'*Candidatus* Endonucleariobacter rarus'	70	0; 2; 31/30.5
Pauci995 (Dirren *et al.* 2014)	AATCTCTTCGGGATCTCTGACATG	*Paucibacter toxinivorans*	70	23; 77; 465/0
Bu154 (this study)	CGAACAGTTATCGCCCACTACC	*Inhella* sp. ectosymbiont of strain G	55	17; 14859; 29751/0
Le827 (this study)	CCCTAAGGCTTCCAACAGCC	'*Candidatus* Ovatusbacter abovo'	60	0; 1; 6/33.3
Del1424 (this study)	GCTCACGCGCTTCTGGCTTATAC	'*Candidatus* Turbabacter delicatus'	70	0; 0; 0/30.7
AlRick85 (this study)	CGTCTGCCACTAACATATGTGAGCT	'*Candidatus* Intestinusbacter nucleariae'	70	0; 0, 1/69.9

[a]Formamide concentrations in the hybridisation buffer.
[b]Number of hits with the 'Probe Match' tool in the RDP database: zero mismatches; one mismatch; two mismatches.
[c]Minimal difference in formamide concentrations between target and non-targets calculated with the 'Mismatch Analysis' tool from mathFISH.

Phylogenetic analyses

The software DNA Baser v3.5.0 (Heracle BioSoft) served as tool for assembling partial sequences. Chimeric sequences were detected and removed using Mallard and Pintail (Ashelford *et al.* 2005). For phylogenetic analyses, the ARB software package (Ludwig *et al.* 2004) with the SILVA database SSU Ref 111 (Pruesse *et al.* 2007) was used.

All available *Nuclearia* 18S rRNA gene sequences from described species, our isolates, and as outgroup two sequences from *Candida* sp. (AB013586 and EU348785) were included for phylogenetic tree reconstruction. Sequences were trimmed and aligned with the MAFFT aligner (Katoh and Standley 2013). Alignments were manually optimized and ambiguous regions (e.g. insertions in the V4, V7 and V8 domains) were removed resulting in 1501 positions with 150 distinct alignment patterns. Another phylogenetic tree including all our *N. delicatula* clones, *N. delicatula* (AF349563) and *N. simplex* (AF349566)/*N. moebiusi* (AF349565) as outgroup was calculated. In addition, sequences were aligned and trimmed as described above but none of the hypervariable regions were removed (2363 positions with 204 distinct alignment patterns).

The 16S rRNA gene sequences of symbionts were aligned with the SINA web aligner (www.arb-silva.de/aligner/). Five phylogenetic trees (*Ca.* Endonucleariobacter rarus: 1305 positions, 56 distinct patterns; ectosymbionts: 1417 positions, 199 distinct patterns; endosymbionts: 1558 positions, 827 distinct patterns; clone library strain G: 1383 positions, 617 distinct patterns; clone library strain D: 1415 positions, 769 distinct patterns) were calculated with our sequences and related sequences from the SILVA database (quality scores $\geq$88).

For the reconstruction of phylogenetic trees, maximum likelihood (ML) and Bayesian inference (BI) methods were used. Bootstrapped ML trees were calculated (1000 iterations) using the RAxML algorithm (Stamatakis, Hoover and Rougemont 2008). The parameters were GTR (general time reversible) model with a Γ distribution for rate heterogeneity among sites, with four discrete rate categories. BI was calculated using the ExaBayes software package (©The Exelixis Lab). The posterior probabilities from BI trees (four chains; 100 000 generations) were added to ML trees where trees of both methods were congruent. Full-length 16S rRNA gene sequences from clone libraries and 18S rRNA gene sequences of the *Nuclearia* strains were deposited in the EMBL database with the accession numbers LN875040–LN875170.

CARD-FISH and probe design

First, CARD-FISH with the general probes EUB I-III (Daims *et al.* 1999), ALF968 (Neef 1997), BET42a, GAM42a (Manz *et al.* 1992), CF319a (Manz *et al.* 1996), HGC69a (Roller *et al.* 1994) and VER47 (Buckley and Schmidt 2001) allowed for the identification of symbionts on a higher taxonomical level. Afterwards clusters of potential symbionts were chosen from phylogenetic trees of the 16S rRNA gene clone libraries. Specific probes were designed based on the sequences of these candidate clusters. Probe design with the dedicated ARB tool resulted in four specific CARD-FISH probes (Table 2). The Ribosomal Database Project (www.rdp.cme.msu.edu) and the web tool Mathfish (Yilmaz, Parnerkar and Noguera 2011) were used for *in silico* testing of the new probes. Appropriate formamide concentrations (for highest stringency) were determined empirically. Non-specific staining was addressed with the probe NON338 (Wallner, Amann and Beisker 1993). CARD-FISH on filters was done with differently labelled tyramids (fluorescein and Alexa546) following the previously published protocol (Dirren *et al.* 2014). In addition, CARD-FISH of amoebae on gelatine-coated glass slides and embedded in agarose were prepared.

Microscopy and photographic documentation

Differential interference and phase contrast images were acquired with a Canon EOS1000D controlled by the software AxioVision 4.8.2 (Zeiss) installed on an Axio Imager.M1 microscope (Zeiss). CARD-FISH preparations were analysed at the same microscope with epifluorescence microscopy (Zeiss optical filter sets: set 01, 10, 14 and 43) and by confocal laser-scanning microscopy (SP5-R, Leica Microsystems, Germany).

Transmission electron microscopy

Glutaraldehyde (final conc. 1.25 %) and osmium tetroxide (final conc. 1 %) were mixed and added to small volumes of *N. delicatula* strain D and strain G cultures (after centrifugation at 1000 g for 20 min and discarding of supernatants). Fixation was done on ice for 1 h followed by two washing steps (centrifugation for 10 min at 2000 g and exchanging of fixative solution with H_2O). Washed pellets were resuspended in melted agar (2 %). After hardening and cutting the agar block into smaller pieces (~10 mm^3), they were block stained with uranylacetat (1 %) for 1 h at room temperature. Subsequently, samples were dehydrated in an ethanol series (70%, 80%, 96% and 100%) and finally in propylenoxide, followed by embedding in epon-araldite. Ultrathin sections were cut with an Ultracut UCT (Leica) and poststained with lead citrate for 6 min. An electron microscope Philips CM100 equipped with a digital camera (Gatan Orius 1000) was used for the analysis of the TEM preparations.

RESULTS AND DISCUSSION

Morphological versus molecular phylogeny of *Nuclearia* spp.

For a long time, nucleariid amoebae were described using only morphological characters. However, the majority of these amoeboid species share many features used for their identification (see table 1 in Yoshida, Nakayama and Inouye 2009). It seems that some inadequately defined characters were even interpreted differently by researchers, e.g. if amoebae may form flattened/spherical cells, if a glycocalyx is present or absent and if the nucleolus is evident. This becomes obvious, when comparing fig. 11 in Patterson (1984), where the author stated the lack of a glycocalyx, with fig. 6 in Pernin (1976), where the presence of EPS was proven. In addition to these 'vague' characters, other features like the formation of multinucleate syncytia, cyst production and the appearance of branched filopodia might be rarely or not at all observed depending on culture and observation conditions. Even the cell size of single isolates may vary depending on culture conditions. We documented at least for one isolate a shrinkage of cells in the course of cultivation. The mean cell size of *N. thermophila* strain D6 decreased from initially 24.6 μm (day 7 after isolation, $n = 56$) to 15.7 μm (day 90, $n = 100$). Thus, most probably these inconsistencies and different interpretations of features led to redescriptions of species and incorrect identifications.

This assumption is additionally supported by the fact that two *N. simplex* isolates clustered in the 18S rRNA gene-based phylogenetic tree very distantly (Fig. 1A) with *N. moebiusi* and

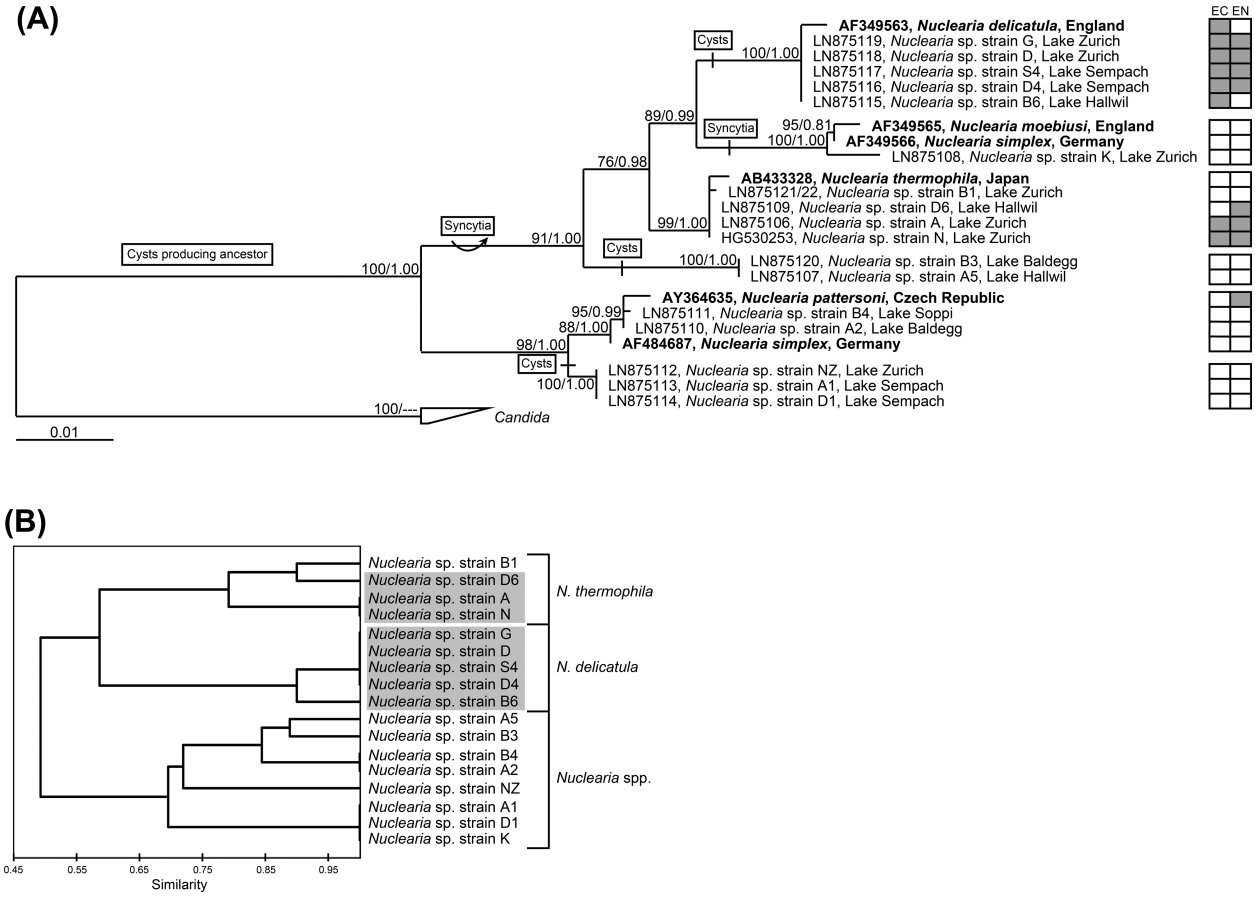

Figure 1. Phylogenetic analysis of the *Nuclearia* spp. isolates. (**A**) 18S rRNA gene based ML tree with posterior probabilities from BI; ML bootstrap value/BI probability. Described *Nuclearia* species are shown in bold and *Candida* was used as outgroup. Hypothetical gain (curved arrow) and loss (bar) of features 'cyst production' (Cysts) and 'formation of syncytia' (Syncytia) are shown. Detected ectosymbionts (EC) and endosymbionts (EN) are indicated with a filled square for the respective isolate. Scale bar: number of nucleotide substitutions per site. (**B**) Cladistic tree based on morphological characters of the *Nuclearia* spp. isolates. *X*-axis: similarity value (Jaccard coefficient). The affiliations of amoeboid isolates to described species are indicated on the right hand. Isolates with associated symbionts are grey shaded.

N. pattersoni, respectively. Because of this discrepancy, we considered the two as *N. simplex* identified isolates to belong to different species. Consequently, we will name these phylogenetic groups as *N. moebiusi* and *N. pattersoni* cluster, respectively. Moreover, two sequences of one and the same *N. moebiusi* isolate (AF349565 and AF484686) were included in phylogenetic trees by some authors (Dykova *et al.* 2003; Yoshida, Nakayama and Inouye 2009) which further caused confusions.

Nevertheless, in this study we partly worked with traditional morphological features for comparisons of our strains (Fig. 2 and Fig. S1, Supporting Information) with published species descriptions. To characterize our *Nuclearia* spp. isolates, we even included four additional features: benthic isolate, pelagic isolate, presence of ectosymbionts and presence of endosymbionts (Table 1). We checked if the morphological classification corresponded to the molecular phylogeny by performing a cladistic analysis based on presence/absence of characters. The cladistic tree (Fig. 1B) and the 18S rRNA gene-based ML tree (Fig. 1A) were in good accordance regarding the *N. delicatula* and the *N. thermophila* clusters. In both trees, they were sister groups including same isolates. In contrast, the third big cluster in the cladistical tree unified isolates from distant branches of the ML tree. Although the substructure of this third cluster reflected quite well the 18S rRNA gene-based phylogeny, two isolates clustered differently. In the cladistic tree, *Nuclearia* sp. strain NZ had no close relative and strain K formed together with strains A1 and D1 a group, which was not confirmed by molecular phylogeny. Taken together, only *N. delicatula* and *N. thermophila* strains could be identified solely by their morphological traits. For the affiliation of all other isolates, additional molecular information (18S rRNA genes) was needed.

Assignment of isolates to described species

The species descriptions of *N. delicatula* from Patterson (1984) and Cann (1986) are in good accordance with morphological features (Table 1) observed for all isolates in the *N. delicatula* cluster.

The morphological features described for *N. moebiusi* differed from what we observed for *Nuclearia* sp. strain K. We found spherical cells as well as a glycocalyx which was not reported for *N. moebiusi*. When considering the 'excavate cavities' (fig. 11 from Patterson 1984) to be the glycocalyx and additionally taking the trait 'spherical form' less restrictive, we can assign our isolate to this species (i.e. *N. moebiusi* strain K).

The morphological incongruences between *N. thermophila* strain N and the original species description of *N. thermophila* by Yoshida, Nakayama and Inouye (2009) were discussed in our previous study (Dirren *et al.* 2014). For the isolates clustering together with *N. thermophila*, we reported a good accordance with the characters earlier described for *N. thermophila* strain N. Only the formation of syncytia could not be documented for strains B1 and D6. The present results including morphological and

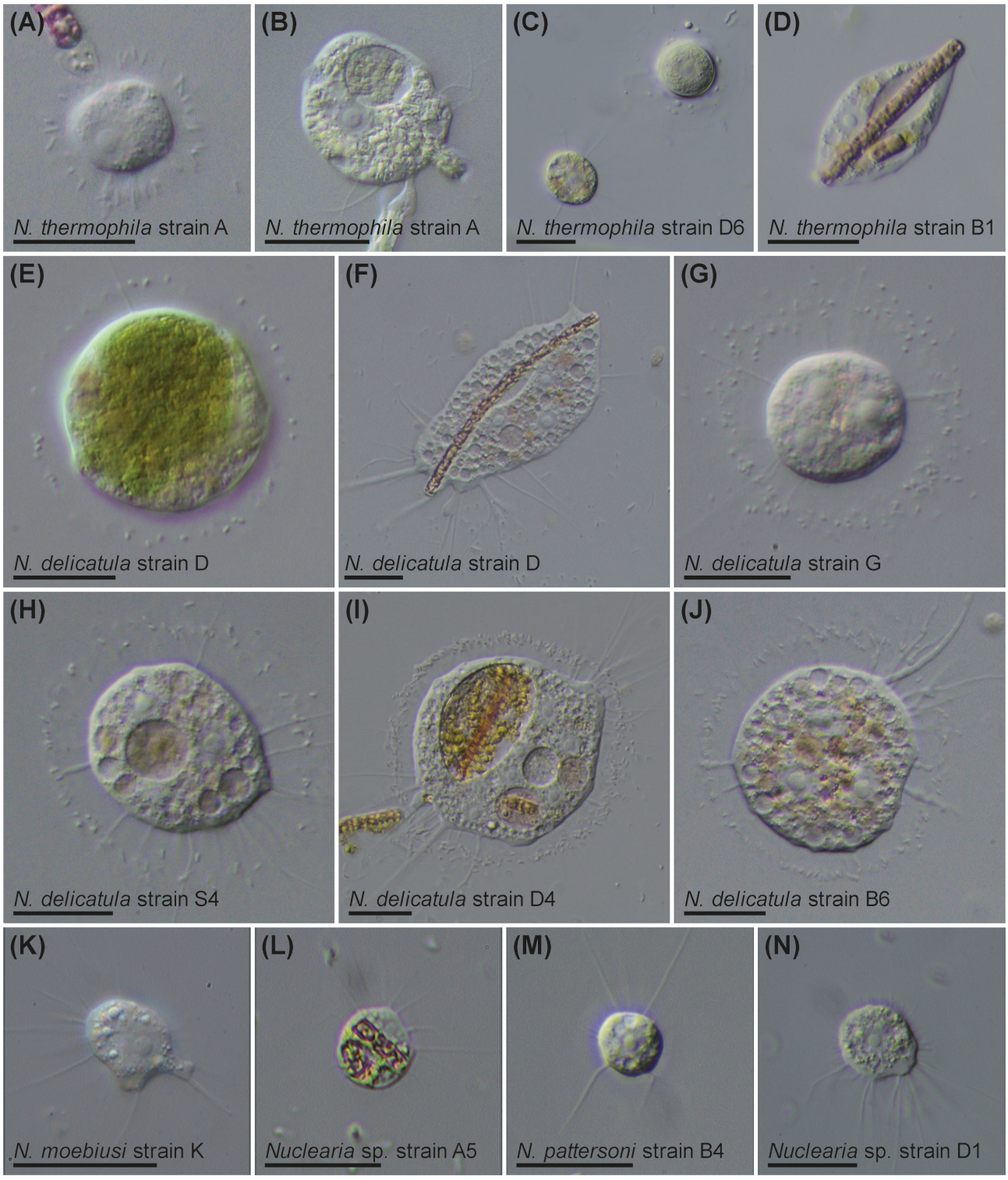

Figure 2. Light microscopical images of 12 *Nuclearia* spp. isolates. (**A**) Nucleariid cell attached to a *P. rubescens* filament surrounded by ectosymbiotic bacteria right after isolation. (**B**) Feeding individual after loss of ectosymbionts (3 months later). (**C**) Vegetative cell (left) and cyst (right) next to each other. (**D**) Elongated organism with phagocytised *P. rubescens* fragments. (**E**) Green cell (due to partly digested pigments of food organisms) colonized by ectosymbiotic bacteria 9 months after isolation. (**F**) Amoeboid multinucleated organism which lost ectosymbionts (3 years later). (**G**) Multinucleate spherical individual with symbiotic bacteria inside the glycocalyx. (**H**) Nearly spherical cell with radiating filopodia. Note food vacuoles and two nucleoli. (**I**) Feeding individual with a large food vacuole containing remnants of *P. rubescens* filaments at different states of digestion. Ectosymbiotic bacteria surround the multinucleate cell. (**J**) Organism partly attached to the surface colonized by symbiotic bacteria. Concentrated filopodia indicate the direction of locomotion. (**K**) Amoeboid cell with a prominent nucleolus. (**L**) Individual with ingested fragments of *P. rubescens*. (**M**) Spherical cell freely floating. (**N**) Amoeboid organism moving on surface. All pictures were taken with differential interference contrast (DIC) and scale bars indicate 20 μm.

phylogenetic analyses of four different isolates (strains B1, D6, A, N) thus justify their assignment to the species *N. thermophila*.

All described features for *N. pattersoni* (Dykova *et al.* 2003) except the presence of endosymbionts could be observed for *Nuclearia* sp. strain B4 and A2. Taking their phylogenetic close relatedness (Fig. 1A) into account, we can assign them to the species *N. pattersoni*.

The isolates *Nuclearia* sp. strain NZ, strain A1 and strain D1 built a sister group to the *N. pattersoni* cluster (Fig. 1A). Morphologically these three isolates were very similar and the lack of cysts was the only character differentiating them from *N. pattersoni* isolates. However, the phylogenetic distance (Fig. 1A) still does not allow for assigning them to the described species.

Finally, the two isolates *Nuclearia* sp. strain B3 and A5 formed a discrete new phylogenetic group. In spite of only minor morphological differences (e.g. formation of syncytia in strain A5) to isolates in the *N. moebiusi* and *N. pattersoni* clusters, we suppose that they form a new species. Phylogenetic reconstruction even points at a rather basal position, probably representing a sister group to *N. delicatula*, *N. moebiusi* and *N. thermophila*. We added hypothetical gains and losses of the features 'cyst production' and 'formation of syncytia' to the corresponding branches (Fig. 1A). The fact that we found cyst production for isolates all over the tree may indicate that the common ancestor was encysting. In contrast, the formation of syncytia was found only for isolates in one of the main branches and thus could be an acquired trait.

Variability of the nucleariid 18S rRNA gene copies

For all but seven *Nuclearia* isolates, PCR amplification of the 18S rRNA gene with general eukaryotic primers and direct sequencing was successful (LN875106–LN875114). In contrast, assembling of partial 18S rRNA gene sequences failed for *N. thermophila* strain B1, *Nuclearia* sp. strain B3 and all *N. delicatula* isolates (strains G, D, S4, D4 and B6). For *N. thermophila* strain B1, a poly-G region causing 'hard stops' during sequencing resulted in two non-overlapping partial sequences. The first part (~700 nt) and the second part (~1230 nt) of the 18S rRNA gene could thus not be assembled. Sequence qualities of all *N. delicatula* strains and *Nuclearia* sp. strain B3 dropped in regions containing homopolymers due to superposition of signals. This pointed to sequence variations in multiple 18S rRNA gene copies (e.g. different lengths of homopolymers). Therefore, PCR products of *N. delicatula* strains and *Nuclearia* sp. strain B3 were cloned and *de novo* sequenced resulting in partial sequences with high-quality scores even for regions containing homopolymers. Two to ten different clones were completely sequenced (LN875123–LN875170) for *N. delicatula* isolates and *Nuclearia* sp. strain B3. In order to exclude that interclone variation was introduced by PCR and sequencing errors, we reamplified 18S rRNA genes from cleaned-up plasmids of three *N. delicatula* strain D4 clones. The obtained sequences were identical to those generated by direct sequencing of inserts. Thus, detected interclone variations most probably originated from natural variations in 18S rRNA gene copies and were not artefacts.

Microheterogeneities in the nucleariid 18S rRNA genes have been already documented by Zettler *et al.* (2001). They mainly originate from size variations in the insertions inside the V4, V7 and V8 domains (sensu De Rijk *et al.* 1992). Pairwise sequence distances were calculated for each clone library of *N. delicatula* strains (G, D, S4, D4), *Nuclearia* sp. strain B3 and *N. thermophila* strain B1 (Fig. S2A, Supporting Information). Variations in the 18S rRNA gene copies of *N. thermophila* strain B1 (mean ± standard deviation: 0.21±0.07 %) were lower than those in *N. delicatula* strains (0.48±0.15 % to 0.63±0.24 %) and in *Nuclearia* sp. strain B3 (0.44±0.24 %). Intrastrain variations (distances of clone sequences: 0.58±0.05 %) were about three times higher than interstrain variations (distances of the consensus sequences: 0.17±0.07 %) for *N. delicatula* isolates. Thus, they could not be separated phylogenetically on the base of this marker gene (Fig. S2B, Supporting Information). When we calculated sequence similarity of *N. delicatula* (AF349563) and *N. delicatula* strain G without these variable parts in the V4, V7 and V8 domains, we got a high value of 99.7 %. In contrast, sequence similarity including the hypervariable stretches was only 94 %. In the same way, 18S rRNA gene copies in single isolates are mainly diverging (e.g. due to insertion and deletion of nucleotides) inside the homopolymers of hypervariable domains. Slipped-strand mispairing (Levinson and Gutman 1987) might be the mechanism behind this phenomenon. A slightly higher mutation rate could also be detected for the variable stretches in sequences from the *N. pattersoni* cluster (e.g. sequence similarity of the described *N. pattersoni* and *N. pattersoni* strain B4: with homopolymer region 99 % and without 99.2 %) but not within the *N. thermophila* cluster. The sequence similarity of *N. thermophila* (AB433328) and *N. thermophila* strain A was 99.6% with and without homopolymer regions.

Taken together, divergence and/or number of 18S rRNA gene copies vary between different *Nuclearia* species. Regarding their mutation rates, homopolymer regions can differ drastically from the rest of the sequence. And finally, accumulations of mutations in these regions seem to be species specific.

Associations of *Nuclearia* spp. with prokaryotes

In total 8 of our 17 isolates were associated with endosymbiotic and/or ectosymbiotic bacteria. Symbionts could be detected for all *N. delicatula* strains but not for *Nuclearia* isolates from three other clusters (Fig. 1A). Beside these homogeneous branches, also mixed groups were found. In the *N. thermophila* cluster, three out of five representatives had symbionts (Fig. 1A). The *N. pattersoni* cluster was also heterogeneous. It was only reported for *N. pattersoni* (Dykova *et al.* 2003) that this amoeba harboured a rickettsial endosymbiont.

The non-systematic appearance of symbiotic associations inside the genus *Nuclearia* indicates a species-dependent disposition. As far as we know such a high variability within a single genus has been described only for *Acanthamoeba* spp. (Fritsche *et al.* 1993; Horn *et al.* 1999; Horn 2008). Either some *Nuclearia* species evolved traits by which the probability to enter a symbiotic relationship increases or it is a plesiomorph character that has been partly lost. Considering their phylogenetic position within opisthokonts, it is of interest to search specifically for such traits in future genetic analysis. Probably, nucleariids have already specific genes and machineries which are involved in selecting and controlling of symbiotic partners (Bosch 2014). The question about the frequency of prokaryotic symbionts in unicellular opisthokonts still remains to be addressed. Today, it is not clear if the lack of knowledge simply derives from the low number of studies looking for symbiotic associations or if the highly diverse interactions inside the genus *Nuclearia* are an exceptional phenomenon.

Nuclearia thermophila isolates and their ectosymbionts

In a previous study (Dirren *et al.* 2014), we identified the ectosymbiont of *N. thermophila* strain N as the betaproteobacterium

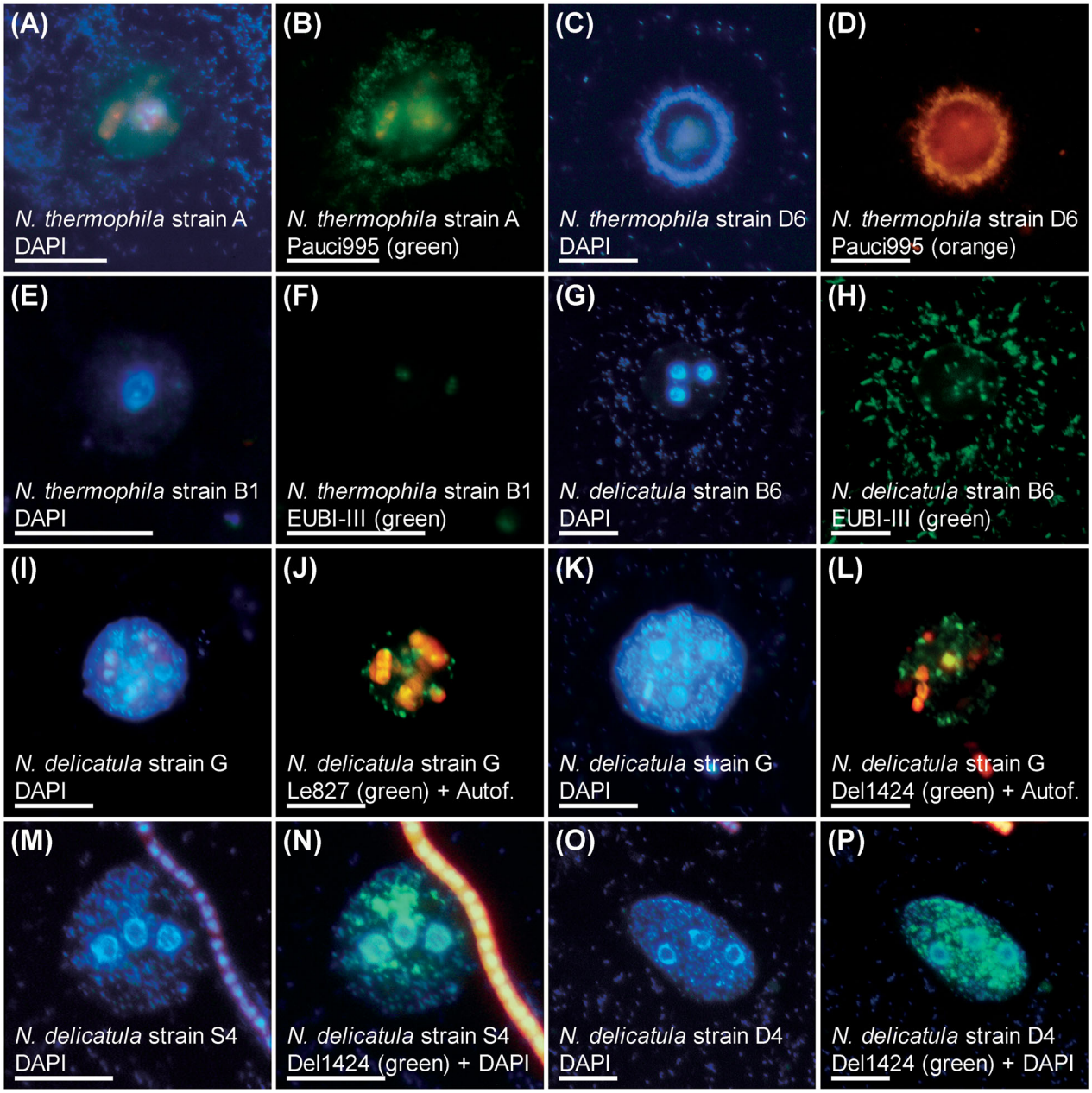

Figure 3. CARD-FISH of bacterial symbionts associated with (**A–F**) *N. thermophila* and (**G–P**) *N. delicatula* isolates. For abbreviations of applied oligonucleotide probes, see Table 2. Different fluorophore-specific filter sets were used to image the cells after hybridization. The first two and the last two columns of each row represent always the same cell. (A) Cell with ingested *P. rubescens* filaments and accompanying bacteria after DAPI staining. (**B**) Ectosymbiotic bacteria hybridized with the probe Pauci995. (**C**) Cell with well-preserved glycocalyx. Ectosymbionts are still arranged close to the cell surface. (**D**) The probe Pauci995 hybridized with ectosymbionts. (**E**) The nucleariid cell stained with DAPI. (F) No endosymbionts detected with the probe EUBI-III. (G) Three nuclei and ectosymbionts observed after DAPI staining. (**H**) No endosymbionts were detected with the probe EUBI-III. (**I**) Nuclei, endosymbionts and ingested *P. rubescens* filaments after DAPI staining. (**J**) Merged picture of the CARD-FISH signal and the autofluorescence. A small part of the endosymbionts are hybridized with the probe Le827. (**K**) Individual with three nuclei, endo- and ectosymbiotic bacteria after DAPI staining. (**L**) Merged picture of the CARD-FISH signal and the autofluorescence. The main part of endosymbionts hybridized with the probe Del1424. (**M**) Nucleariid cell with three nuclei and endosymbionts attached to a *P. rubescens* filament. (**N**) Merged picture of the CARD-FISH and the DAPI signal. One part of the endosymbiotic bacteria is hybridized with the probe Del1424. (**O**) Individual with three nuclei, endosymbionts and accompanying bacteria after DAPI staining. (**P**) Merged picture of the CARD-FISH and the DAPI signal. The major part of endosymbionts are hybridized with the probe Del1424. Scale bars represent 20 μm.

P. toxinivorans (Rapala *et al.* 2005) and designed the specific CARD-FISH probe 'Pauci995' (Table 2). Within the *N. thermophila* cluster, only strain A of our new isolates was also associated with ectosymbiotic bacteria right after isolation (Fig. 2A). Unfortunately during cultivation, these bacteria got lost (Fig. 2B) before CARD-FISH filters could be prepared. Although cells were surrounded by a glycocalyx, no ectosymbionts were observed for strain D6 (Fig. 2C; Fig. S1C, Supporting Information) and strain B1 (Fig. 2D). Since the ectosymbiont of strain N (*P. toxinivorans* strain SD41) was available as pure culture, we checked if the other strains could be infected with these bacteria. When we added an aliquot (1 ml) of a pure bacterial culture to the medium of ectosymbiont-free isolates, we observed a colonization of strains A and D6 (Fig. 3A–D). Surprisingly, this was not the case for strain B1. This

experiment indicated a highly specific interaction of *P. toxinivorans* strain SD41 with only one phylotype of the *N. thermophila* cluster (strain D6, A and N; see Fig. 1A). The fact that the ectosymbiont did not colonize the glycocalyx of the close relative strain B1 points to a distinct contribution of the host to this symbiosis.

The importance of a glycocalyx has been most extensively investigated for epithelial cells of the gastrointestinal tract (Moran, Gupta and Joshi 2011). The composition of glycoproteins produced by the host determines the physical (e.g. viscosity) and chemical (e.g. site for bacterial adhesion) nature of this extracellular structure and thus the interaction with bacteria. On the other hand, the composition of the glycocalyx can be modulated by bacteria in distinct ways (Hooper and Gordon 2001). This suggests a cross-talk between host and bacteria mediated by the glycocalyx. Furthermore, in the early branching metazoan *Hydra*, receptors, species-specific antimicrobial peptides (Bosch 2014) and even viruses (Bosch, Grasis and Lachnit 2015) have been shown to be main factors shaping the ectosymbiotic bacterial community. Unfortunately, the molecular interactions between the *N. thermophila* strains and *P. toxinivorans* are yet not studied.

Nuclearia thermophila isolates and their endosymbionts

In the *N. thermophila* cluster, three (A, D6 and N) out of four isolates harboured the gammaproteobacterial endosymbiont *Ca.* Endonucleariobacter rarus (Fig. 4A–H and Dirren *et al.* 2014). Hybridization with the specific probe CoNuc67 (Table 2) resulted in positive signals from all bacteria in strains A and D6 (Fig. 4C, G–H). In contrast, endosymbionts were missing in strain B1 (Fig. 3E and F) which additionally had a slightly divergent 18S rRNA gene sequence (Fig. 1A).

Interestingly, 18S rRNA gene sequences of strains D6, A and N were identical, but 16S rRNA gene sequences of their endosymbiont *Ca.* Endonucleariobacter rarus were slightly different. Endosymbionts of strains D6 and A formed a sister group to bacteria of strain N (Fig. 5A), although strains A and N were isolated from the same lake, and strain D6 from a 25 km distant lake.

Nuclearia delicatula isolates and their ectosymbionts

Four of our *N. delicatula* strains (D, G, S4 and D4) had both ectosymbionts (Figs 2E–I and 4Q–T) and endosymbionts (Figs 3I–P and 4I–P). Strain B6 was only associated with ectosymbionts (Figs 2J and 3G–H). Based on the 16S rRNA gene clone library of strain G (Fig. S3A, Supporting Information), three specific oligonucleotide probes were designed: Bu154, Le827 and Del1424 (Table 2). Ectosymbionts of strain G could be hybridized with the betaproteobacterial probe Bu154 (Fig. 4Q–T). The closest described relative (98.6% sequence similarity) to the cluster covered by this probe was *Inhella inkyongensis* (Song *et al.* 2009). Phylogeny of nucleariid's ectosymbionts (Fig. 5B) highlights that these ectosymbiotic bacteria are related (95.5% sequence similarity) to the earlier identified ectosymbiont of *N. thermophila* strain N (*P. toxinivorans*). *Inhella* sp. and *P. toxinivorans* have both sequence divergences to the bacteriochlorophyll *a* containing bacteria *Roseateles* (Suyama *et al.* 1999) and *Rubrivivax* (Willems, Gillis and De Ley 1991) of ~4% and ~5%, respectively. They form a metabolically diverse group sometimes referred to as '*Sphaerotilus-Leptothrix* group' (Spring 2006; Song *et al.* 2009) inside the family Comamonadaceae. As far as we know, a symbiotic live style has not been reported for any representative of this group.

Nucleariid amoebae are conspicuous concerning their nutrition: they can feed on harmful filamentous cyanobacteria, without being affected by toxic secondary metabolites (Dirren *et al.* 2014). In the previous study, we showed that *P. toxinivorans* was able to degrade microcystins, the cyanobacterial toxins stored in food organisms. In the case of *Inhella* sp., we have yet no proof for any similar metabolic capability. However, the spatial proximity to the host's cell surface suggests an exchange of metabolites between the symbiotic partners.

Nuclearia delicatula isolates and their endosymbionts

The gammaproteobacterial probe Le827 and the deltaproteobacterial probe Del1424 gave positive CARD-FISH signals for intracellular bacteria of *N. delicatula* strain G and no signals from bacteria in the cultivation medium. Endosymbionts hybridized with probe Le827 specific for a cluster of gammaproteobacteria were evenly distributed and represented a small part of total bacteria inside the cells (Figs 3I–J and 4P). Because of the homogenous distribution and their estimated abundance by CARD-FISH, we could assign this phylotype to distinct morphological features (morphotype 1) observed on TEM pictures (Fig. 6A and B). Bacteria had two membranes of a typical Gram-negative cell wall and an electron dense spot inside cells (Fig. 6C and D). They were localized in the cytoplasm and mostly surrounded by an electron translucent halo but never by an additional membrane. Some intracellular bacteria observed in *N. radians* display remarkable morphological similarities to bacteria in *N. delicatula* strain G (see Plate 4c from Cann and Page 1979). No described relatives of our endosymbiotic bacteria could be found in public databases. Apart from some sequences of uncultured gammaproteobacteria (highest sequence similarity 94.3%), the closest relatives were *Candidatus* Berkiella aquae (88.5% sequence similarity) and *Candidatus* Berkiella cookevillensis (88.1% sequence similarity) (Fig. 5C). These bacteria were found after infection inside the nucleus of *Acanthamoeba polyphaga* (Mehari *et al.* 2016). We never detected bacteria inside the nuclear membrane of strain G and endosymbionts differed morphologically from the recently characterized symbionts (Mehari *et al.* 2016, e.g. no electron dense spot). The 16S rRNA gene sequences of these symbiotic bacteria and strain G's endosymbiont are too much diverged to resolve their phylogenetic relationship based solely on this marker gene. Thus, corresponding branches had to be collapsed (low support values) in the phylogenetic tree (Fig. 5C). We propose the taxonomic status '*Candidatus* Ovatusbacter abovo' for the endosymbiont of *N. delicatula* strain G.

Double hybridization with the gammaproteobacterial probe Le827 and the deltaproteobacterial probe Del1424 showed different endosymbionts in strain G being hybridized (Fig. 4P). In contrast to the even distribution and low frequency of bacteria labelled with Le827, endosymbionts hybridized with Del1424 showed a lumped occurrence and were highly abundant (Figs 3K–L and 4P). These characteristics corresponded to the other prominent morphological phenotype (morphotype 2) seen on TEM pictures (Fig. 6A and B). Cells had again a typical Gram-negative cell wall structure (Fig. 6E and F) but in contrast to '*Candidatus* Ovatusbacter abovo' they were always surrounded by an additional host-derived membrane. Small vacuole-like structures harboured single cells (Fig. 6G and H) or multiple bacteria of morphotype 2 (Fig. 6E and F). We even detected these endosymbionts inside food vacuoles, often attached to the membrane of the vacuole, together with remnants of the food organism *P. rubescens* (Fig. 6B, G and H). In contrast to cyanobacterial cells, endosymbiotic bacteria seemed to be resistant to

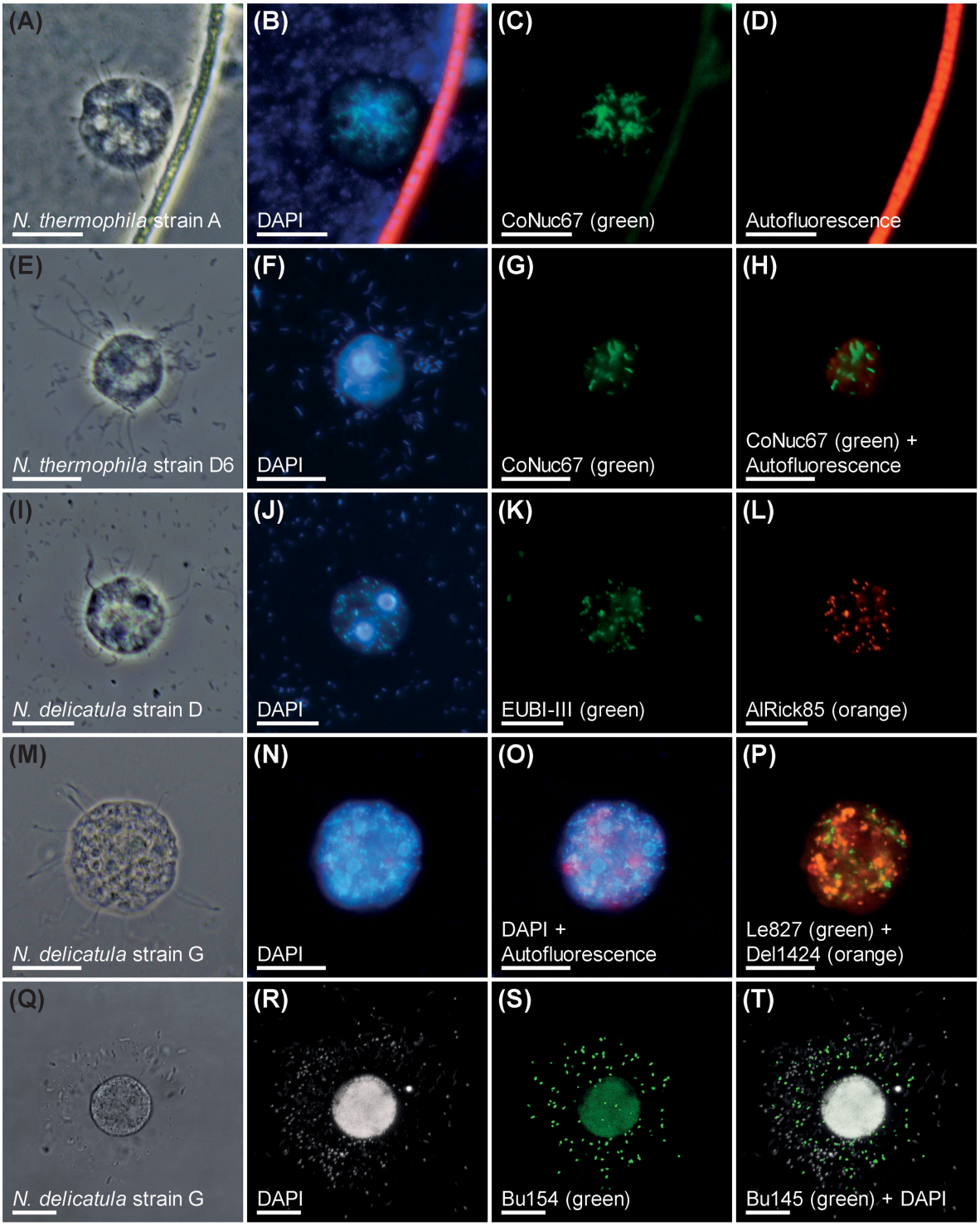

Figure 4. CARD-FISH preparations of (**A–H**) *N. thermophila* and (**I–T**) *N. delicatula* isolates embedded in (A–P) gelatine and (**Q–T**) agarose. Single nucleariid cells of different isolates are shown after hybridization. For abbreviations of applied oligonucleotide probes, see Table 2. Always the same cell is depicted in one row. Light microscopical pictures are placed in the first column; further columns represent epifluorescence images taken with fluorophore-specific filter sets. Pictures (Q–T) were recorded with a confocal laser scanning microscope. (A) Nucleariid cell next to a *P. rubescens* filament. (**B**) Endosymbiotic and accompanying bacteria after DAPI staining. (**C**) All endosymbionts hybridized with the probe CoNuc67. (**D**) Strong autofluorescence of the phototrophic cyanobacterium *P. rubescens*. (**E**) Cell with radiating filopodia. (**F**) Nucleus and bacteria stained with DAPI. (**G**) Hybridization of all endosymbionts with the probe CoNuc67. (**H**) Merged picture of autofluorescence (originating from ingested *P. rubescens*) and the CARD-FISH signal. (**I**) Nucleariid cell with two nuclei. (**J**) Endosymbionts visible after DAPI staining. (**K**) The oligonucleotide probe EUBI-III hybridized with endosymbionts and bacteria in the cultivation medium. (**L**) All endosymbionts hybridized specifically with the probe AlRick85. (**M**) Spherical cell with radiating filopodia. (**N**) Three nuclei and bacterial endosymbionts stained with DAPI. (**O**) Merged picture of autofluorescence (*P. rubescens* in food vacuoles) and DAPI. (**P**) Double hybridization with the two probes Le827 (few scattered bacteria) and Del1424 (many bacteria and lumped distribution). (**Q**) Spherical *Nuclearia* cell embedded in agarose. (**R**) Bacteria surrounding the cell stained with DAPI. (**S**) Ectosymbiotic bacteria hybridized with the probe Bu154. (**T**) Merged pictures of hybridized and DAPI-stained organisms. Scale bars represent 20 μm.

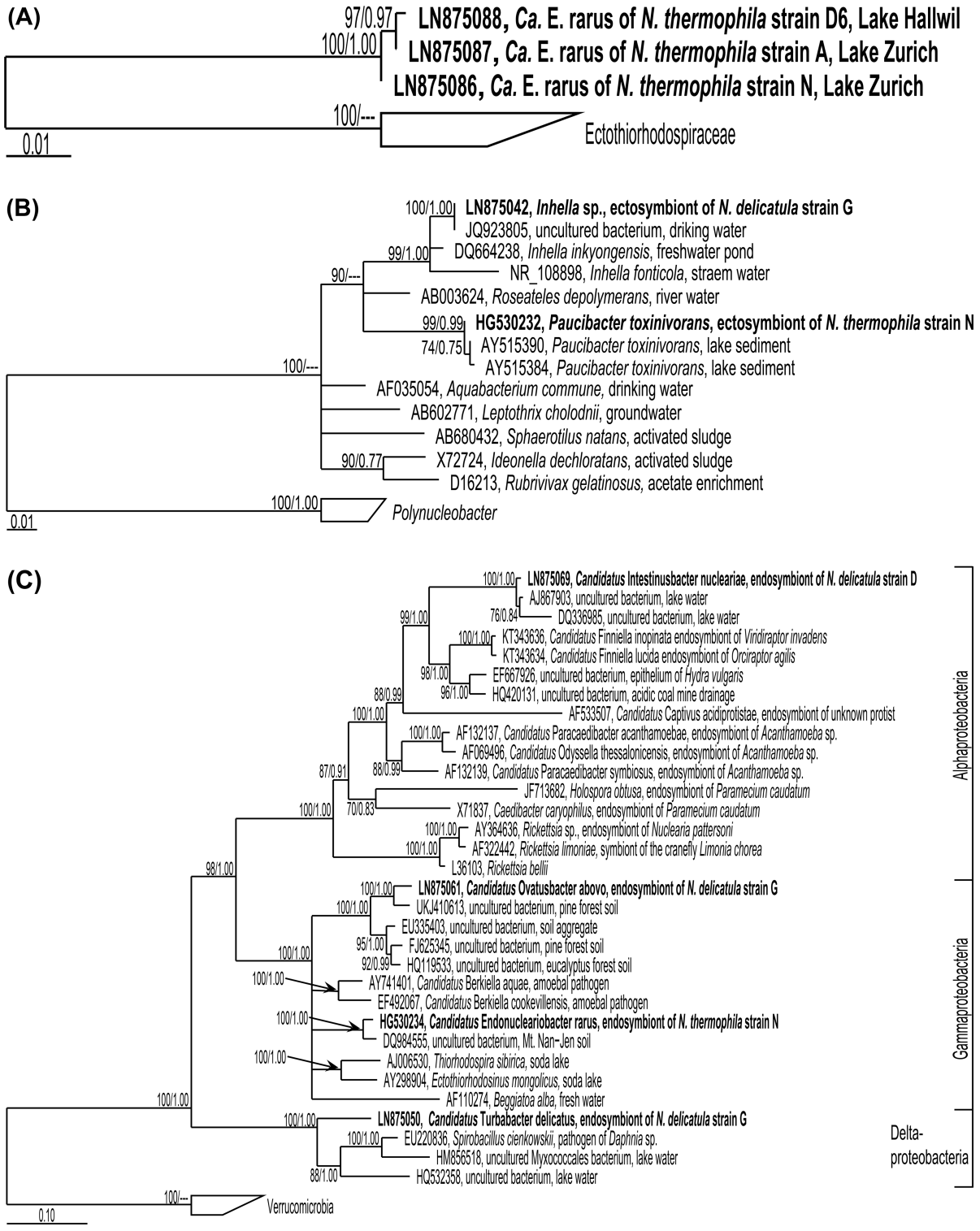

Figure 5. Phylogenetic analyses of (**A**) *Candidatus* Endonucleariobacter rarus, (**B**) ectosymbionts and (**C**) endosymbionts based on their 16S rRNA genes. Symbionts of *Nucleaia* spp. are shown in bold. ML trees with posterior probabilities from BI; ML Bootstrap value/BI probability. Branches with bootstrap values ≤60 were collapsed. Scale bars: numbers of substitutions per site. Ectothiorhodospiraceae, *Polynucleobacter* and Verrucomicrobia were used as outgroups, respectively.

digestion. This observation in combination with the fact that the deltaproteobacterial probe Del1424 did not hybridize with bacteria in the cultivation medium speaks against a possible role of these intracellular bacteria as food.

Usually bacterial pathogens are taken up by phagocytosis and then either prevent the fusion of lysosomes (e.g. *Legionella pneumophila*; Roy and Kagan 2000) or escape the phagosomes (e.g. *Rickettsia prowazekii*; Whitworth *et al.* 2005). Because of the facts that cyanobacterial cells were digested in food vacuoles and endosymbionts were never seen freely in the cytoplasm, there is no indication for any of these two strategies. TEM pictures of *A. castellanii* infected with the pathogenic symbiont

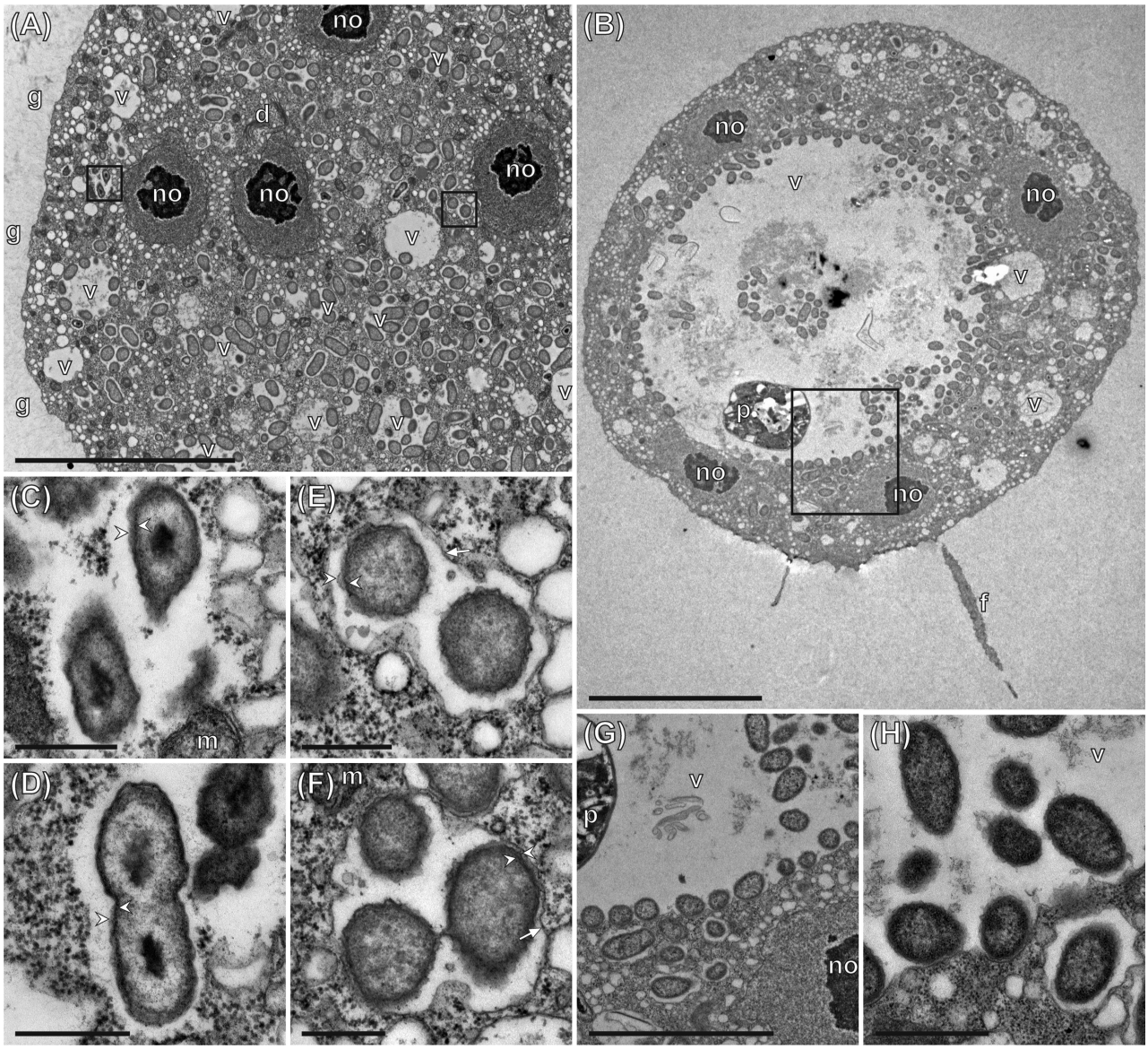

Figure 6. TEM images of *N. delicatula* strain G. (**A** and **B**) Overview of two different nucleariid cells displaying nuclei with their nucleoli (no) and numerous bacteria inside their cytoplasm. Magnifications of squares are shown in (**C**), (**E**) and (**G**), respectively. Two morphotypes of endosymbiotic bacteria can be distinguished. The less abundant morphotype 1 can be found freely inside the cytoplasm, whereas the prominent morphotype 2 is present in vacuole-like structures (v). (C) Two bacteria and (**D**) a dividing individual of morphotype 1 inside the nucleariid cell. A characteristic central electron-dense spot and a typical Gram-negative cell wall structure with two membranes (arrowheads) are visible. No peribacterial membrane is present, but an electron translucent halo surrounds the cell. (E and **F**) Cells having the characteristics of morphotype 2 are tightly packed inside a peribacterial membrane (arrow). The Gram-negative cell wall organization with two membranes (arrowheads) is visible. The cell content of this endosymbiont has a homogenous appearance on TEM pictures. (G) In the big central food vacuole (see overview B), an intact *P. rubescens* filament (p) and remnants of digested cyanobacteria can be seen. In addition to the food organism, bacteria of the morphotype 2 are present inside the food vacuoles (v). Many bacteria seem to be attached to the membrane. Additionally, single or few cells of this morphotype are enclosed in membranes apparently not connected to the food vacuole. (**H**) Higher magnification of the interface between food vacuole and cytoplasm. Bacteria of the morphotype 2 are attached to the membrane sometimes forming cavities. Bacteria seem to be intact and not digested. d, dictyosome; f, filopodium; g, glycocalyx; m, mitochondrion; no, nucleolus; p, *P. rubescens* filament; v, vacuole-like structures. Scale bars represent 10 μm in (A and B), 4 μm in (G), 1 μm in (H) and 500 nm in (C–F).

'*Candidatus* Jidaibacter acanthamoeba' (fig. 1 in Schulz *et al.* 2015) resemble conspicuously our observations of the frequent endosymbiont. In contrast to this accordance, types of the symbioses seem to differ. The regular exponential growth of the host *N. delicatula* speaks against a severe pathogenic nature of its endosymbiotic bacteria. Again, no close relatives of this endosymbiont belonging to the deltaproteobacteria were found in public databases. The closest relative (89.8% sequence similarity) was a pathogenic bacterium of daphnids named *Spirobacillus cienkowskii* (Rodrigues *et al.* 2008). None of the sequences included in the phylogenetic tree (Fig. 5C) clustered together with this endosymbiont of strain G. Thus, we propose the taxonomic status '*Candidatus* Turbabacter delicatus' for these bacteria. Specific hybridization with the deltaproteobacterial probe Del1424 showed that the endosymbiont was also present in cells of strains S4 and D4 (Fig. 3M–P). Like in strain G, not all of the intracellular bacteria were labelled. In contrast to the positive hybridization with the gammaproteobacterial probe Le827 with the other part of endosymbionts in strain G, no signal was obtained for strains S4 and D4. Most probably, these strains

additionally harboured other so far unidentified endosymbiotic bacteria.

The specific alphaproteobacterial probe AlRick85 was designed based on a cluster of sequences in the 16S rRNA gene clone library of *N. delicatula* strain D (Fig. S3B, Supporting Information). AlRick85 hybridized specifically with all endosymbiotic bacteria of this isolate (Fig. 4I–L). In public databases, no closely related sequences were found except for some uncultured bacteria. The closest characterized relatives were *Candidatus* Finniella inopinata (89.1% sequence similarity) and *Candidatus* Finniella lucida (88.4% sequence similarity) which are rickettsial endosymbionts of viridiraptorid amoeboflagellates (Fig. 5C). Sequences of the alphaproteobacterial endosymbiont of strain D affiliated with the recently established family *Candidatus* Paracaedibacteraceae (Hess, Suthaus and Melkonian 2016). This family is formed by endosymbionts of different protists. So far they were found in Rhizaria, Excavata and Amoebozoa. Here we report for the first time a representative of this family inside an opisthokont protist. TEM pictures proved that only one bacterial morphotype was found in the cytoplasm (Fig. 7A): Gram-negative bacterial cells with invaginated cell walls which were surrounded by an electron translucent halo (Fig. 7B and C). No additional host-derived membrane or electron-dense layer (which was observed for the endosymbionts of the viridiraptorid amoeboflagellates) was detected for this endosymbiont. The observed features were consistent with the descriptions for the members of the family *Candidatus* Paracaedibacteraceae. Because of a distinct phylogenetic clustering, several morphological differences and a new host habitat, we propose the provisional name '*Candidatus* Intestinusbacter nucleariae' for these endosymbiotic bacteria.

Description of '*Candidatus* Ovatusbacter abovo' (Gammaproteobacteria)

Etymology: L. masc. adj. *ovatus*, egg-shaped; N.L. masc. n. *bacter*, a rod; N.L. masc. n. *Ovatusbacter*, egg-shaped bacterium, inspired by the appearance on cross-sections (TEM), when cells looked like fried eggs. L. prefix. *ab*, from; L. nt. dat. sing. n. *ovo* of *ovum*, egg; L. *abovo* (*ab ovo*) mythological allusion to one of the two eggs of Leda which was the primary cause of the Trojan War; expression used to indicate an ancient origin.

Rod-shaped bacterium up to 1 μm in length (mean length: 0.65 μm and mean width: 0.34 μm; $n = 30$) with a typical Gram-negative cell wall structure and a characteristic central electron-dense spot observed by TEM. Basis of assignment: 16S rRNA gene sequence (accession number: LN875061) and positive signal with the specific CARD-FISH probe Le827 (5′-CCCTAAGGCTTCCAACAGCC-3′). So far only detected in the cytoplasm of *N. delicatula* strain G (accession number: LN875119), isolated from Lake Zurich (47°19′11.5″N, 8°33′10.1″E), Switzerland. Typically 50–200 cells could be observed inside this nucleariid host. Uncultured so far.

Description of '*Candidatus* Turbabacter delicatus' (Deltaproteobacteria)

Etymology: L. fem. n. *turba*, noisiness, swarm, mass; N.L. masc. n. *bacter*, a rod; N.L. masc. n. *Turbabacter*, rod-shaped bacterium appearing in masses. L. masc. adj. *delicatus*, spoilt, delicate, referring to the host species *N. delicatula* and to its lifestyle in a protected nutrient-rich niche.

Rod-shaped Gram-negative bacterium up to 1.69 μm in length (mean length: 1 μm and mean width: 0.48 μm; $n = 30$).

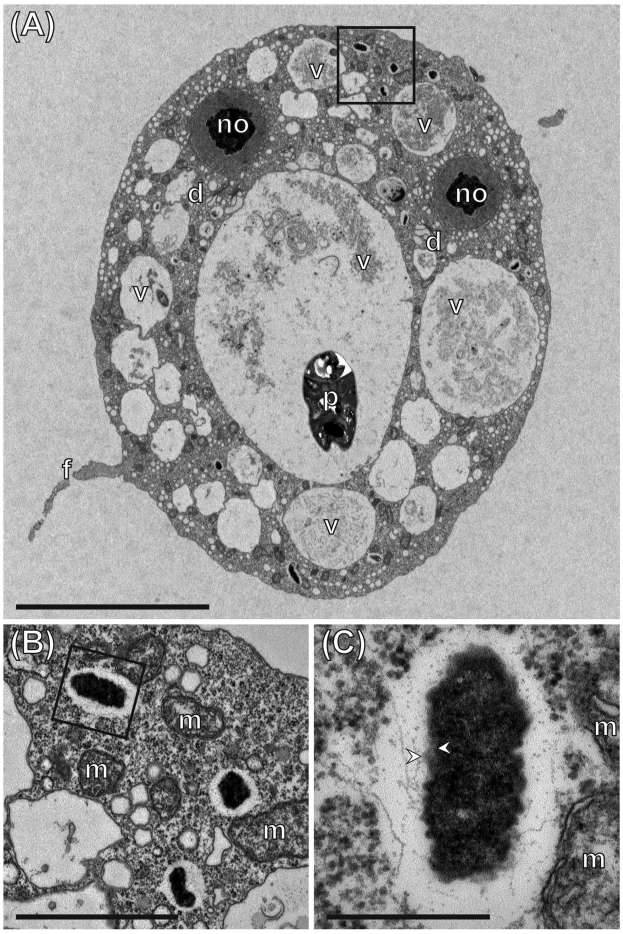

Figure 7. TEM images of *N. delicatula* strain D. (**A**) Overview showing the highly vacuolated (v) nucleariid cell with two prominent nucleoli (no) and a filopodium (f). Inside the big central food vacuole, a *P. rubescens* filament (p) and remnants of already digested cyanobacterial cells are visible. Only one morphotype of endosymbionts with homogenous electron-dense cell content is present. (**B**) Higher magnification of three endosymbionts (square in A). Bacteria are located freely in the cytoplasm surrounded by a pronounced electron-translucent halo. (**C**) Higher magnification of one bacterial cell (square in B). No peribacterial membrane but two membranes (arrowheads) of the Gram-negative cell wall are visible. d, dictyosome; f, filopodium; m, mitochondrion; no, nucleolus; p, *P. rubescens* filament; v, vacuole-like structures. Scale bars represent 10 μm in (A), 2 μm in (B) and 500 nm in (C).

Cells are found inside vacuole-like structures and food vacuoles (often attached to the membrane) but never freely in the cytoplasm. Basis of assignment: 16S rRNA gene sequence (accession number: LN875050) and positive signal with the specific CARD-FISH probe Del1424 (5′-GCTCACGCGCTTCTGGCTTATAC-3′). Up to now detected in three different *N. delicatula* isolates: strain G, strain S4 and strain D4 (accession numbers: LN875119, LN875117 and LN875116). Usually several hundreds of individuals were observed inside the host species which were isolated from two Swiss Lakes: Lake Zurich (47°19′11.5″N, 8°33′10.1″E) and Lake Sempach (47°08′15.8″N, 8°08′25.8″E). Uncultured so far.

Description of '*Candidatus* Intestinusbacter nucleariae' (Rickettsiales, Alphaproteobacteria)

Etymology: L. masc. adj. *intestinus*, internal; N.L. masc. n. *bacter*, a rod; N.L. masc. n. *Intestinusbacter*, rod-shaped bacterium

living internal (inside eukaryotic cells). N.L. fem. gen. sing. n. *nuclleariae* from *Nuclearia*, taxonomic name of the single genus *Nuclearia* within the family Nucleariidae, indicating the affiliation of the host.

Rod-shaped bacterium up to 1.1 μm in length (mean length: 0.71 μm and mean width: 0.29 μm; $n = 18$) with Gram-negative invaginated cell wall organization and translucent halo (on conventional TEM pictures). Basis of assignment: 16S rRNA gene sequence (accession number: LN875069) and positive signal with the specific CARD-FISH probe AlRick85 (5′-CGTCTGCCACTAACATATGTGAGCT-3′). So far only detected in the cytoplasm of *N. delicatula* strain D (accession number: LN875118), isolated from Lake Zurich (47°19′11.5″N, 8°33′10.1″E), Switzerland. Uncultured so far.

SUPPLEMENTARY DATA

Supplementary data are available at FEMSEC online.

ACKNOWLEDGEMENTS

We thank Jakob Pernthaler (University of Zurich), Gianna Pitsch (University of Zurich) and Sebastian Hess (Dalhousie University) for fruitful discussions and Marvin Moosmann for the help with the isolation of amoebae. TEM imaging was performed with equipment and support of the Centre for Microscopy, University of Zurich.

FUNDING

This study was financed by the Swiss National Science Foundation (SNF 31003A_138473 and SNF 31003A_159842).

Conflict of interest. None declared.

REFERENCES

Alegado RA, King N. Bacterial influences on animal origins. *Cold Spring Harb Perspect Biol* 2014;**6**:a016162.

Artari A. Morphologische und biologische Studien über *Nuclearia delicatula* Cienk. *Zool Anz* 1889;**12**:408–16

Ashelford KE, Chuzhanova NA, Fry JC *et al.* At least 1 in 20 16S rRNA sequence records currently held in public repositories is estimated to contain substantial anomalies. *Appl Environ Microb* 2005;**71**:7724–36.

Bosch TC. Rethinking the role of immunity: lessons from *Hydra*. *Trends Immunol* 2014;**35**:495–502.

Bosch TC, Grasis J, Lachnit T. Microbial ecology in *Hydra*: Why viruses matter. *J Microbiol* 2015;**53**:193–200.

Buckley DH, Schmidt TM. Environmental factors influencing the distribution of rRNA from Verrucomicrobia in soil. *FEMS Microbiol Ecol* 2001;**35**:105–12.

Cann JP. The feeding behavior and structure of *Nuclearia delicatula* (Filosea: Aconchulinida). *J Protozool* 1986;**33**:392–6.

Cann JP, Page FC. *Nucleosphaerium tuckeri* nov. gen. nov. sp.- A new freshwater filose amoeba without motile form in a new family Nucleariidae (Filosea: Aconchulinida) feeding by ingestion only. *Arch Protistenk* 1979;**122**:226–40.

Casadevall A. Evolution of intracellular pathogens. *Annu Rev Microbiol* 2008;**62**:19–33.

Daims H, Bruhl A, Amann R *et al.* The domain-specific probe EUB338 is insufficient for the detection of all Bacteria: development and evaluation of a more comprehensive probe set. *Syst Appl Microbiol* 1999;**22**:434–44.

De Rijk P, Neefs J-M, Van De Peer Y *et al.* Compilation of small ribosomal subunit RNA sequences. *Nucleic Acid Res* 1992;**20**:2075–89.

Dirren S, Salcher MM, Blom JF *et al.* Ménage-à-trois: The amoeba *Nuclearia* sp. from Lake Zurich with its ecto- and endosymbiotic bacteria. *Protist* 2014;**165**:745–58.

Dykova I, Veverkova M, Fiala I *et al.* *Nuclearia pattersoni* sp. n. (Filosea), a new species of amphizoic amoeba isolated from gills of roach (*Rutilus rutilus*), and its rickettsial endosymbiont. *Folia Parasitol* 2003;**50**:161–70.

Franzenburg S, Walter J, Künzel S *et al.* Distinct antimicrobial peptide expression determines host species-specific bacterial associations. *P Natl Acad Sci USA* 2013;**110**:E3730–8.

Fraune S, Anton-Erxleben F, Augustin R *et al.* Bacteria-bacteria interactions within the microbiota of the ancestral metazoan *Hydra* contribute to fungal resistance. *ISME J* 2015;**9**:1543–56.

Fraune S, Bosch TC. Long-term maintenance of species-specific bacterial microbiota in the basal metazoan *Hydra*. *P Natl Acad Sci USA* 2007;**104**:13146–51.

Freeman MF, Gurgui C, Helf MJ *et al.* Metagenome mining reveals polytheonamides as posttranslationally modified ribosomal peptides. *Science* 2012;**338**:387–90.

Fritsche TR, Gautom RK, Seyedirashti S *et al.* Occurrence of bacterial endosymbionts in *Acanthamoeba* spp. isolated from corneal and environmental specimens and contact lenses. *J Clin Microbiol* 1993;**31**:1122–6.

Gast RJ, Sanders RW, Caron DA. Ecological strategies of protists and their symbiotic relationships with prokaryotic microbes. *Trends Microbiol* 2009;**17**:563–9.

Hess S, Suthaus A, Melkonian M. '*Candidatus* Finniella' (Rickettsiales, Alphaproteobacteria), novel endosymbionts of viridiraptorid amoeboflagellates (Cercozoa, Rhizaria). *Appl Environ Microb* 2016;**82**:659–70.

Hooper LV, Gordon JI. Glycans as legislators of host–microbial interactions: spanning the spectrum from symbiosis to pathogenicity. *Glycobiology* 2001;**11**:1R–10R.

Horn M. Chlamydiae as symbionts in eukaryotes. *Annu Rev Microbiol* 2008;**62**:113–31.

Horn M, Fritsche TR, Gautom RK *et al.* Novel bacterial endosymbionts of *Acanthamoeba* spp. related to the *Paramecium caudatum* symbiont *Caedibacter caryophilus*. *Environ Microbiol* 1999;**1**:357–67.

Huttenhower C, Gevers D, Knight R *et al.* Structure, function and diversity of the healthy human microbiome. *Nature* 2012;**486**:207–14.

Katoh K, Standley DM. MAFFT multiple sequence alignment software version 7: improvements in performance and usability. *Mol Biol Evol* 2013;**30**:772–80.

Kiers ET, West SA. Evolving new organisms via symbiosis. *Science* 2015;**348**:392–4.

Kikuchi Y, Hayatsu M, Hosokawa T *et al.* Symbiont-mediated insecticide resistance. *P Natl Acad Sci USA* 2012;**109**:8618–22.

Lema KA, Bourne DG, Willis BL. Onset and establishment of diazotrophs and other bacterial associates in the early life history stages of the coral *Acropora millepora*. *Mol Ecol* 2014;**23**:4682–95.

Levinson G, Gutman GA. Slipped-strand mispairing: a major mechanism for DNA sequence evolution. *Mol Biol Evol* 1987;**4**:203–21.

Liu Y, Steenkamp ET, Brinkmann H *et al.* Phylogenomic analyses predict sistergroup relationship of nucleariids and Fungi and paraphyly of zygomycetes with significant support. *BMC Evol Biol* 2009;**9**:272.

Lozupone CA, Stombaugh JI, Gordon JI *et al.* Diversity, stability and resilience of the human gut microbiota. *Nature* 2012;**489**:220–30.

Ludwig W, Strunk O, Westram R *et al.* ARB: a software environment for sequence data. *Nucleic Acid Res* 2004;**32**:1363–71.

McFall-Ngai M, Hadfield MG, Bosch TC *et al.* Animals in a bacterial world, a new imperative for the life sciences. *P Natl Acad Sci USA* 2013;**110**:3229–36.

Manz W, Amann R, Ludwig W *et al.* Phylogenetic oligodeoxynucleotide probes for the major subclasses of proteobacteria: problems and solutions. *Syst Appl Microbiol* 1992;**15**:593–600.

Manz W, Amann R, Ludwig W *et al.* Application of a suite of 16S rRNA-specific oligonucleotide probes designed to investigate bacteria of the phylum cytophaga-flavobacter-bacteroides in the natural environment. *Microbiol-UK* 1996;**142**:1097–106.

Mehari YT, Hayes BJ, Redding KS *et al.* Description of '*Candidatus* Berkiella aquae' and '*Candidatus* Berkiella cookevillensis', two intranuclear bacteria of freshwater amoebae. *Int J Syst Evol Micr* 2016;**66**:535–41.

Moon-van der Staay SY, De Wachter R, Vaulot D. Oceanic 18S rDNA sequences from picoplankton reveal unsuspected eukaryotic diversity. *Nature* 2001;**409**:607–10.

Moran AP, Gupta A, Joshi L. Sweet-talk: role of host glycosylation in bacterial pathogenesis of the gastrointestinal tract. *Gut* 2011;**60**:1412–25.

Muyzer G, Ramsing NB. Molecular methods to study the organization of microbial communities. *Water Sci Technol* 1995;**32**:1–9.

Nakayama T, Marin B, Kranz HD *et al.* The basal position of scaly green flagellates among the green algae (Chlorophyta) is revealed by analyses of nuclear-encoded SSU rRNA sequences. *Protist* 1998;**149**:367–80.

Neef A. Anwendung der In-situ-Einzelzell-Identifizierung von Bakterien zur Populationsanalyse in komplexen mikrobiellen Biozönosen. *Ph.D. Thesis*, Technische Universität München 1997.

Ouwerkerk JP, de Vos WM, Belzer C. Glycobiome: bacteria and mucus at the epithelial interface. *Best Pract Res Cl Ga* 2013;**27**:25–38.

Paracer S, Ahmadjian V. *Symbiosis: An Introduction to Biological Associations*. New York: Oxford University Press, 2000.

Patterson DJ. The genus *Nuclearia* (Sarcodina, Filosea): Species composition and characteristics of the taxa. *Arch Protistenk* 1984;**128**:127–39.

Pernin P. Study in vivo of an ameoba with pseudopodes filosa: *Nuclearia simplex* Cienkowski 1865 (Protozoa, Rhizopodea, Filosia, Aconchulinida). *Protistologica* 1976;**12**:555–62.

Pruesse E, Quast C, Knittel K *et al.* SILVA: a comprehensive online resource for quality checked and aligned ribosomal RNA sequence data compatible with ARB. *Nucleic Acid Res* 2007;**35**:7188–96.

Rapala J, Berg KA, Lyra C *et al.* *Paucibacter toxinivorans* gen. nov., sp nov., a bacterium that degrades cyclic cyanobacterial hepatotoxins microcystins and nodularin. *Int J Syst Evol Microbiol* 2005;**55**:1563–8.

Rodrigues JLM, Duffy MA, Tessier AJ *et al.* Phylogenetic characterization and prevalence of '*Spirobacillus cienkowskii*,' a red-pigmented, spiral-shaped bacterial pathogen of freshwater *Daphnia* species. *Appl Environ Microb* 2008;**74**:1575–82.

Rodríguez-Ezpeleta N, Brinkmann H, Burey SC *et al.* Monophyly of primary photosynthetic eukaryotes: green plants, red algae, and glaucophytes. *Curr Biol* 2005;**15**:1325–30.

Roller C, Wagner M, Amann R *et al.* *In situ* probing of gram-positive bacteria with high DNA G + C content using 23S rRNA targeted oligonucleotides. *Microbiol-UK* 1994;**140**:2849–58.

Roy CR, Kagan JC. *Evasion of Phagosome Lysosome Fusion and Establishment of a Replicative Organelle by the Intracellular Pathogen Legionella Pneumophila*. Austin: Landes Bioscience, 2000.

Schulz F, Martijn J, Wascher F *et al.* A rickettsiales symbiont of amoebae with ancient features. *Environ Microbiol* 2015, DOI: 10.1111/1462-2920.12881.

Smith JM. Generating novelty by symbiosis. *Nature* 1989;**341**:284–5.

Song J, Oh HM, Lee JS *et al.* *Inhella inkyongensis* gen. nov., sp. nov., a new freshwater bacterium in the order Burkholderiales. *J Microbiol Biotechn* 2009;**19**:5–10.

Spring S. The genera Leptothrix and Sphaerotilus. In: Dworkin M, Falkow S, Rosenberg E *et al.* (eds.) *The Prokaryotes*. New York: Springer, 2006, 758–77.

Stamatakis A, Hoover P, Rougemont J. A rapid bootstrap algorithm for the RAxML web servers. *Syst Biol* 2008;**57**:758–71.

Steenkamp ET, Wright J, Baldauf SL. The protistan origins of animals and fungi. *Mol Biol Evol* 2006;**23**:93–106.

Suyama T, Shigematsu T, Takaichi S *et al.* *Roseateles depolymerans* gen. nov., sp. nov., a new bacteriochlorophyll a-containing obligate aerobe belonging to the beta-subclass of the Proteobacteria. *Int J Syst Bacteriol* 1999;**49**:449–57.

Thrash JC, Boyd A, Huggett MJ *et al.* Phylogenomic evidence for a common ancestor of mitochondria and the SAR11 clade. *Sci Rep* 2011;**1**:13, DOI: 10.1038/srep00013.

Wallner G, Amann R, Beisker W. Optimizing fluorescent *in situ* hybridization with rRNA-targeted oligonucleotide probes for flow cytometric identification of microorganisms. *Cytometry* 1993;**14**:136–43.

Walsby AE, Avery A, Schanz F. The critical pressures of gas vesicles in *Planktorhrix rubescens* in relation tothe depth of winter mixing in Lake Zurich, Switzerland. *J Plankton Res* 1998;**20**:1357–75.

Whitworth T, Popov VL, Yu X-J *et al.* Expression of the *Rickettsia prowazekii pld* or *tlyC* gene in *Salmonella enterica* serovar typhimurium mediates phagosomal escape. *Infect Immun* 2005;**73**:6668–73.

Willems A, Gillis M, De Ley J. Transfer of *Rhodocyclus gelatinosus* to *Rubrivivax gelatinosus* gen. nov., comb. nov., and phylogenetic relationships with *Leptothrix*, *Sphaerotilus natans*, *Pseudomonas saccharophila*, and *Alcaligenes latus*. *Int J Syst Evol Micr* 1991;**41**:65–73.

Wylezich C, Karpov SA, Mylnikov AP *et al.* Ecologically relevant choanoflagellates collected from hypoxic water masses of the Baltic Sea have untypical mitochondrial cristae. *BMC Microbiol* 2012;**12**:1–13.

Yilmaz LS, Parnerkar S, Noguera DR. mathFISH, a web tool that uses thermodynamics-based mathematical models for *in silico* evaluation of oligonucleotide probes for fluorescence *in situ* hybridization. *Appl Environ Microb* 2011;**77**:1118–22.

Yoshida M, Nakayama T, Inouye I. *Nuclearia thermophila* sp. nov. (Nucleariidae), a new nucleariid species isolated from Yunoko Lake in Nikko (Japan). *Europ J Protistol* 2009;**45**:147–55.

Zettler LAA, Nerad TA, O'Kelly CJ *et al.* The nucleariid amoebae: more protists at the animal-fungal boundary. *J Eukaryot Microbiol* 2001;**48**:293–7.